Powder Technology 278 (2015) 211–222

Contents lists available at ScienceDirect

Powder Technology

journal homepage: www.elsevier.com/locate/powtec

Characterizing 3D granular flow structures in a double screw mixer using X-ray particle tracking velocimetry

Todd A. Kingston *, Taylor A. Geick, Teshia R. Robinson, Theodore J. Heindel

Department of Mechanical Engineering, Iowa State University, Ames, IA 50011, USA

ARTICLE INFO

Article history:
Received 8 August 2014
Received in revised form 23 November 2014
Accepted 27 February 2015
Available online 15 March 2015

Keywords:
Granular flow
Mixing
Residence time
Screw mixer
X-ray particle tracking velocimetry

ABSTRACT

Granular flows are commonly encountered in many industrial processes, but are difficult to characterize due to the opaque nature of the flow. For instance, screw pyrolyzers are being developed for the thermochemical conversion of biomass into bio-oil, but the granular flow and mixing process inside the reactor lacks fundamental understanding. In this study, X-ray particle tracking velocimetry (XPTV) is used to qualitatively and quantitatively characterize the three-dimensional (3D) granular flow structures in a double screw mixer, which geometrically replicates double screw pyrolyzers, by visualizing the position and speed profiles and quantifying the dimensionless pathlength and dimensionless residence time of individual tracer particles. The influence of screw rotation speed, dimensionless screw pitch, screw rotation orientation, and material injection configuration are investigated. Certain operating conditions are shown to significantly influence the granular flow structures and, in some instances, cause the double screw mixer to behave similar to two single screw conveyors. Comparisons with previous granular mixing studies are made to provide a link between granular flow behavior and mixing effectiveness.

1. Introduction

Granular flows are encountered in many industries including food processing, pharmaceutical production, and energy generation. However, the ability to accurately characterize the three-dimensional (3D) granular flow structures is difficult due to the opaque nature of the flow. A commonly used approach to studying granular flows is through surface visualization via qualitative optical methods [1,2] or quantitative digital image analysis [3–7].While surface visualization has the advantage of being noninvasive, compared to invasive sampling techniques, it does not allow the 3D granular flow to be quantified.

Uchida and Okamoto [8] developed an X-ray penetration image analysis technique to track the movement of a crowd of tungsten tracer particles inside a single screw powder feeder. Image processing techniques were used to quantify the diffusion coefficient by determining the image pixel distribution of the tracer crowd for four different shaped screws. This technique enabled visualization of the opaque powder flow, but did not provide 3D characterization since it featured a single X-ray source and a 2D imaging device. Quantifying the diffusion coefficient using the image pixel distribution is analogous to traditional residence time distribution (RTD) theory that has been used extensively to characterize continuous granular mixing processes [9–11]. RTD theory relies on the injection of numerous tracer particles into the mixing process and requires samples to be collected upon exiting the mixer at discrete points in time. The concentration of tracer particles at these discrete points in time provides the RTD. While the RTD does provide a global assessment of the granular mixing processes, local characterization throughout the mixing processes is unobtainable. Thus, significant effort has gone into developing noninvasive visualization and quantification methods which allow for 3D characterization of opaque flows [12,13].

One noninvasive measurement technique that has shown promise is X-ray particle tracking velocimetry (XPTV), which has been used to characterize multiphase flows [14–17] and granular flows [18]. XPTV provides the ability to characterize opaque flows and offers a good balance between spatial and temporal resolution [17]. Moreover, recent developments by Kingston et al. [19] showed that using a cone-beam compensated back-projection algorithm enabled XPTV to be performed more accurately by eliminating significant errors associated with many prior XPTV methods which utilized a parallel-beam back-projection algorithm.

XPTV provides the ability to thoroughly characterize granular flows, which currently lack fundamental understanding. For example, double screw pyrolyzers are being used for the thermochemical conversion of biomass into bio-oil. The screw pyrolyzer's resulting bio-oil yields are significantly influenced by the screw pyrolyzer's ability to mechanically mix low density biomass particles (e.g., red oak chips, ground corncobs, switchgrass, etc.) with high density inert heat carrier media (e.g., stainless steel shot, refractory sand, etc.). Many research efforts have focused on relating the screw pyrolyzer's operating conditions (e.g., reactor

* Corresponding author.
E-mail addresses: kingston.todd@gmail.com (T.A. Kingston), tgeick@iastate.edu (T.A. Geick), teshiar@iastate.edu (T.R. Robinson), theindel@iastate.edu (T.J. Heindel).

http://dx.doi.org/10.1016/j.powtec.2015.02.061
0032-5910/

temperature) to the resulting products [20–23], but minimal effort has been directed toward understanding the granular flow and mixing process inside the screw pyrolyzer due to the challenges associated with visualizing and quantifying the granular flow.

The goal of this study is to use XPTV to characterize the granular flow inside a double screw mixer, which geometrically resembles screw pyrolyzers currently being used in the biomass thermochemical conversion industry [20]. This goal will be realized through the following objectives: (i) thoroughly characterize the 3D granular flow structures inside the double screw mixer by qualitatively visualizing the tracer particle position and speed profiles, (ii) investigate the influence that changing operating conditions have on the resulting granular flow structures, and (iii) quantitatively determine the dimensionless pathlength and dimensionless residence time of the tracer particle. These results will then be compared to previous granular mixing studies to provide a link between granular flow behavior and mixing effectiveness.

2. Experimental procedures

2.1. Equipment

2.1.1. Screw mixer

Granular studies were performed in the laboratory-scale double screw mixer shown in Fig. 1. The screw mixer features two intermeshing noncontact screws with a screw diameter of D = 2.54 cm. Screw one and two are positioned on the left-hand and right-hand sides, respectively, when viewing the screw mixer from the inlet ports to the outlet ports. A Lin Engineering Silverpak 23CE stepper motor was used to rotate the screws at the desired screw rotation speed. The screw mixer's housing is semi-transparent in both the optical and X-ray spectrums. The housing features a profile which contours to the screws, and was constructed using an additive manufacturing process (i.e., 3D printing). Two material injection ports are positioned in the top of the housing and allow different granular material types and tracer particles to be injected. A series of outlet ports are positioned in the bottom of the housing at the opposite end of the screw mixer, relative to the inlet ports, and allow the granular material to exit under the force of gravity. The effective mixing length is measured from the centerline of the downstream injection port (port two) to the beginning of the outlet ports, and provides a dimensionless mixing length of L/D = 10. The screw mixer's design geometrically replicates the design of double screw pyrolyzers used in the biomass thermochemical conversion industry [20]. Additional details regarding the screw mixer's design can be found in Kingston and Heindel [1,2].

In this study, the effect of four parameters are investigated: (i) screw rotation speed at levels of ω = 20, 40, and 60 rpm (corresponding to Froude numbers, $Fr = \omega^2 D/2g$, of Fr = 0.0057, 0.0227, and 0.0511, respectively, where ω, D, and g are the screw rotation speed, screw diameter, and acceleration due to gravity, respectively); (ii) dimensionless screw pitch at levels of p/D = 0.75, 1.25, and 1.75, where p is the screw pitch and D is the screw diameter; (iii) screw rotation orientation at levels of co-rotating (CoR), counter-rotating up-pumping (CtrR UP), and counter-rotating down-pumping (CtrR DP), where up-pumping and down-pumping refer to the direction of the material flow between the two screws [2]; and (iv) material injection configuration at levels of the red oak chips and glass beads being injected into port one and two, and port two and one, respectively. In this study, each of the parameters were investigated by changing the level of one factor while holding all others constant, resulting in eight different operating conditions, as shown in Table 1.

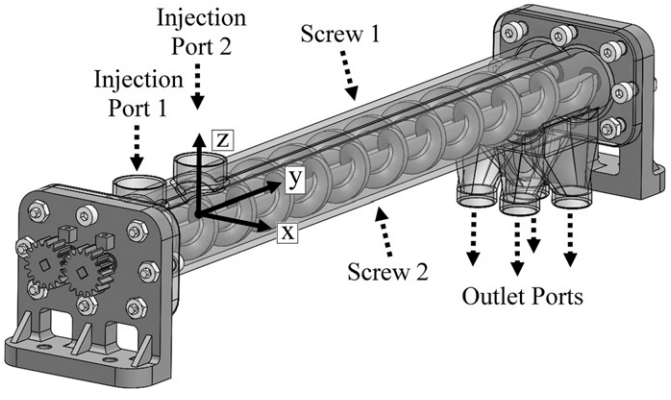

Fig. 1. The screw mixer that was used to perform X-ray particle tracking velocimetry (XPTV) studies.

Previous granular mixing optimization studies by Kingston and Heindel [2] determined that the counter-rotating down-pumping screw orientation was the single most important parameter, and when combined with a screw rotation speed of ω = 60 rpm, a dimensionless screw pitch of p/D = 1.75, and a material injection configuration featuring the red oak chips and glass beads injected into port one and two, respectively, resulted in the best mixing performance, as indicated by the composition variance, of all 54 possible operating conditions within their test range. Thus, this operating condition was chosen as the "reference condition" (operating condition 7 in Table 1) in this study, to which all other operating conditions will be compared.

Additional parameters that were held constant in this study include a 10:1 glass beads to red oak chips mass flow rate ratio, established because of its relevance in the biomass thermochemical conversion industry, and a 65% volumetric fill ratio, which is recommended for screw conveying applications [24]. To satisfy these two parameters, the mass flow rates of the two granular material types were carefully determined for each combination of screw rotation speed and dimensionless screw pitch [1].

2.1.2. X-ray flow visualization facility

X-ray stereography was performed in the X-ray Flow Visualization (XFloViz) Facility at Iowa State University. Two X-ray source/detector pairs were used to simultaneously capture two independent X-ray radiographic projections, which were then coupled together to enable X-ray stereographic imaging. Each X-ray source is a liquid-cooled LORAD LPX200 portable cone-beam source. In this study, X-ray sources one and two featured voltage and current configurations of 150 kV and 3.1 mA, and 140 kV and 3.5 mA, respectively. A single 0.61 mm copper filter was placed in front of each X-ray source to absorb the low energy X-rays prior to entering the imaging region. Both detectors were identical Precise Optics PS164X image intensifiers which feature a 40.6 cm diameter input phosphor and 3.5 cm diameter output phosphor. Coupled to the image intensifiers are two identical DVC-1412 12-bit, monochrome, charge-coupled device (CCD) cameras which have a resolution of 1388 × 1024. However, to improve light sensitivity and increase imaging speed, a 2 × 2 binning configuration, where the signals from adjacent pixels are added together, was used in addition to some cropping, ultimately resulting in an effective resolution of 640 × 512. Using this binning configuration, the cameras captured images in 55 ± 0.5 ms increments resulting in an effective frame rate of 18.2 frames per second (FPS) and the image exposure time for both cameras was 5 ms. The X-ray source/detector pairs were mounted at 90° relative to one another about the central vertical axis in the XFloViz Facility to provide two independent radiographic projections of the screw mixer. In this study, the position of the X-ray source/detector pairs were held at a constant 45° relative to the screw mixer's axial direction, as shown in Fig. 2. This enabled the entire effective mixing region to be visualized. Additional details regarding the XFloViz Facility's equipment and capabilities are available in the literature [19,25].

Table 1
The screw mixer's operating conditions and corresponding levels of parameters that were tested in this study.

Operating condition	Screw rotation speed ω [rpm]	Dimensionless screw pitch p/D [−]	Screw rotation orientation [−]	Material injection configuration RO, GB [−]
1	20	1.75	CtrR DP	1, 2
2	40	1.75		1, 2
3	60	0.75		1, 2
4		1.25		1, 2
5		1.75	CoR	1, 2
6		1.75	CtrR UP	1, 2
7[a]		1.75	CtrR DP	1, 2
8		1.75		2, 1

[a] Reference condition.

2.2. Granular materials

A binary mixture of red oak chips and glass beads were mixed inside the screw mixer. The red oak chips (Fig. 3a) had a particle size ranging from 500 to 6350 μm and an average true density, measured with a pycnometer, of 1350 kg m^{-3}. The glass beads (Fig. 3b) had a particle size ranging from 300 to 500 μm and a true density of 2510 kg m^{-3}. The granular materials are metered into the screw mixer by two independent Tecweigh CR5 volumetric auger feeders. The granular materials are conveyed horizontally by the volumetric feeders, and then free-fall through a vertical injection tube into the screw mixer's material injection ports.

To accurately characterize the dynamic granular mixing processes inside the screw mixer, the tracer particles needed to resemble the granular materials being used in the screw mixer in terms of particle size, shape, and density. Additionally, they needed to provide a large enough X-ray attenuation contrast to be easily identifiable. It was determined from previous studies that the best representation for the actual granular mixing process was the use of "modified" red oak chips [19]. The modification process consisted of soaking a small number of randomly selected red oak chips in a 58% by mass solution of potassium iodide and water for 24 h, and then allowing them to dry for 48 h. Five coats of silver paint (more specifically, pure silver particles in an acrylic lacquer based carrier) were then applied to the outside surface of the red oak chips. Lastly, a single coat of acrylic paint (i.e., fingernail polish) was applied to increase the visual contrast between the tracer particles and the other red oak chips, allowing for extraction and reuse. The combination of potassium iodide and silver paint resulted in a much higher X-ray absorbing tracer particle, while only increasing the average true density of the tracer particles to 1570 kg m^{-3}. The tracer particles were introduced into the red oak chip's material injection inlet stream prior to being injected into the screw mixer.

2.3. X-ray particle tracking velocimetry

2.3.1. X-ray stereography

X-ray stereography couples the two independent 2D X-ray radiographs together, and enables the 3D location of the tracer particle to be determined. Fig. 2 illustrates the X-ray stereography process. One X-ray source/detector pair provides the u–w coordinate of the tracer particle as a function of time, while the other X-ray source/detector pair provides the v–w coordinate as a function of time. In this study, the location of the tracer particle on image one and two for each frame was determined manually for two reasons: (i) the relatively low X-ray attenuation contrast between the tracer particle and the surrounding objects prevented traditional thresholding particle detection methods from being used [17], and (ii) the tracer particles are not rotation invariant, meaning the tracer particle's geometric projection of its shape onto the two detectors is dependent on its orientation, which prevents the use of normalized cross-correlation methods [18].

2.3.2. Tracer particle position

From the two independent but temporally synced X-ray radiographic projections, the 3D coordinate of the tracer particle is obtained as a function of time by using a cone-beam compensated back-projection algorithm that was implemented by Kingston et al. [19]. A cone-beam back-projection algorithm is needed because the X-ray sources are cone-beam sources and, as demonstrated by Kingston et al. [19], failure to compensate for the cone-beam X-ray geometry results in significant error in the tracer particle position.

To improve the visualization and interpretation of the data, a convenient X-ray coordinate system was chosen. The origin was repositioned to the mid-plane between the two screws ($x = 0$), the beginning of the effective mixing region ($y = 0$), and the mid-plane of the screw shafts ($z = 0$), as shown in Fig. 1. To allow for the ability for scale-up and comparison with other mixers, the y-direction, which represents the axial direction of the screw mixer, will be expressed in terms of the dimensionless mixing length, L/D.

An uncertainty analysis was performed for all the experimental tests conducted in this study. The uncertainty in the 3D location of the X-ray equipment was combined with the uncertainty in the cone-beam back-projection algorithm using a root sum of squares (RSS) procedure. The uncertainty was calculated for each tracer particle at each location within the screw mixer. The uncertainty in the tracer particle's location ranged from ±3.1 mm to ±3.7 mm, with an average uncertainty of ±3.2 mm. The average uncertainty represents only 1.3% of the screw mixer's effective mixing length, but 6.4% and 11.2% of the screw mixer width and height, respectively.

2.3.3. Tracer particle speed

Quantifying the speed of the granular materials inside the screw mixer is critical to characterizing the granular flow. After determining the tracer particle's position as a function of time, the x, y, and z components of the velocity were calculated via numerical differentiation using a central difference method outlined by Dos Passos [26] (the x-component of the velocity equation is shown here):

$$V_x(t) \approx \frac{x(t+\Delta t) - x(t-\Delta t)}{2\Delta t} \quad (1)$$

where $x(t+\Delta t)$ is the x-position of the tracer particle at time $t+\Delta t$, $x(t-\Delta t)$ is the x-position of the tracer particle at time $t-\Delta t$, and Δt is the incremental time between successive frames (55 ms in this study).

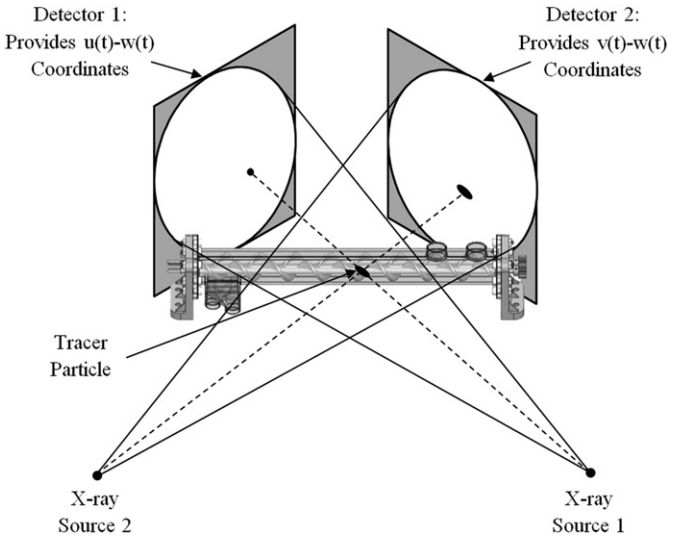

Fig. 2. X-ray stereography schematic indicating the placement of the X-ray source/detector pairs around the screw mixer.

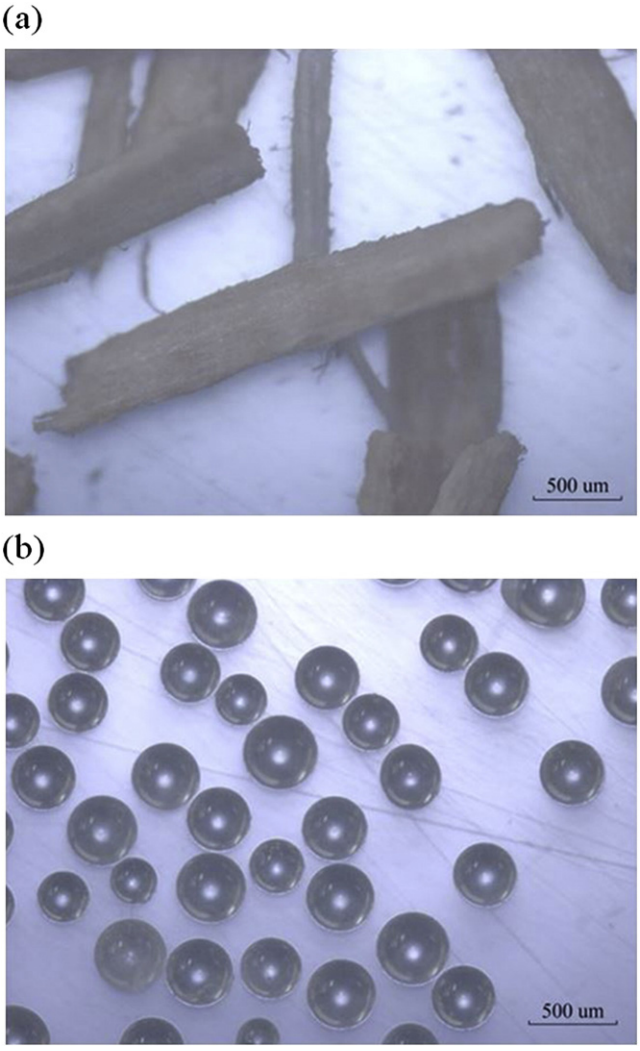

Fig. 3. Magnified images of (a) 500–6350 μm red oak chips and (b) 300–500 μm glass beads, respectively.

In continuous granular mixing processes, defining a transverse and axial speed aids in visualizing the granular dynamics and helps to interpret the effects that changing operating conditions have on the granular flow structures. The transverse speed used in this study is defined as the combination of the x and z velocity components, which are perpendicular to the axis of screw rotation (i.e., y-axis):

$$S_T = \sqrt{V_x^2 + V_z^2} \tag{2}$$

where V_x and V_z are the x- and z-components of the tracer particle's velocity. The transverse speed is always positive per its definition thus the term speed is used. The axial speed is simply defined as the magnitude of the y-component of the velocity:

$$S_A = \sqrt{V_y{}^2}. \tag{3}$$

Since the tracer particle speed was calculated by numerically differentiating the tracer particle position, some inherent noise is generated in the speed data set causing the visualization of the speed data to be slightly more complicated. To aid in removing some of this noise and improve the visualization methods while still maintaining the distinct tracer particle speed characteristics, the LOESS algorithm that was originally proposed by Cleveland [27] and further developed by Cleveland and Devlin [28] was applied to the speed data (i.e., transverse and axial speed), but was not applied to the position data. Additional details of the LOESS algorithm and its implementation into tracer particle visualization is available in the literature [19].

2.3.4. Dimensionless pathlength

The length of the tracer particle pathline throughout the mixing region is a parameter of primary concern due to its ability to quantify the amount of convective mixing taking place inside the screw mixer. However, many granular flow visualization methods cannot provide this important characterization due to the opaque nature of the flow. XPTV provides the 3D position of the tracer particle as a function of time, thus allowing the tracer particle pathlength to be determined. The length of the 3D tracer particle pathline throughout the effective mixing region is determined and then normalized by the screw diameter to provide a dimensionless tracer particle pathlength, L_p/D. This definition results in a minimum dimensionless pathlength equal to the effective mixing region (i.e., minimum $L_p/D = L/D$) but an upper limit does not exist. In fact, as the dimensionless pathlength increases, the movement of the tracer particle in the plane perpendicular to the axial direction (transverse plane) increases, thereby indicating the amount of convective mixing taking place inside the screw mixer. Thus, it is proposed that a longer dimensionless pathlength would lead to an increased mixing effectiveness.

2.3.5. Dimensionless residence time

The residence time of granular material is another critical parameter in many granular mixing applications. For example, in the thermochemical conversion industry, the residence time of individual biomass particles has a significant influence on heat transfer characteristics and resulting products [29]. In this study, the residence time of the tracer particle in the effective mixing region was determined from the time stamps when the tracer particle was located at $L/D = 0$ and $L/D = 10$. However, a dimensionless residence time, defined as the product of the screw rotation speed and the residence time, ωt, is often more desirable and is used in this study.

3. Results and discussion

To demonstrate the qualitative 3D visualization of the tracer particle tracking and the repeatability of the results, the position and speed profile for the reference condition, which was deemed the optimized operating condition by Kingston and Heindel [2] in terms of the mixing effectiveness of the screw mixer, will first be presented, followed by some general discussion of the granular flow structures. Next, a quantitative comparison of the dimensionless pathlength and dimensionless residence time for the different levels of each parameter will be presented and compared to the reference condition. For selected operating conditions, those deemed important based on quantitative results, the position and speed profiles will be presented to provide deeper insight into the reasons leading to deviations from reference condition.

3.1. Reference condition

To fully characterize the 3D granular flow structures inside the screw mixer, the tracer particle position and speed profiles must be visualized simultaneously. To enable this visualization method, a common axis was chosen. The y-axis, which represents the axial direction of the screw mixer, was chosen as this common axis, and is represented in terms of the dimensionless mixing length, L/D, as shown in Fig. 4. The x–z, x–y, and y–z projections of the screw mixer are shown in Fig. 4. With the exception of the x–z projection, the tracer particle moves in the direction of increasing y–direction, which is shown from left to right in Fig. 4. The origin of the screw mixer was conveniently located at the mid-plane between the two screws ($x = 0$), the beginning of the effective mixing region ($L/D = 0$, also $y = 0$), and the mid-plane

of the screw shafts ($z = 0$). The curved profile surrounding the x–z projection represents the inside surface of the screw mixer's housings, and is provided for reference. The arrows above the x–z projection indicate the screw rotation orientation for the given operating condition. The vertical lines on the left and right edge of the x–y and y–z projection represent an axial distance ranging from $L/D = -1$ to $L/D = 10$ and the horizontal lines on the top and bottom edge represent the inside surface of the screw mixer's housing at its highest and lowest points. A faint line drawing of the screws is shown in the x–y and y–z projections to help orient the reader and provide reference to the screw mixer's geometry. However, it must be noted that during testing, the screws were rotating; thus, the position of the tracer particle relative to the position of the screws is irrelevant.

The two plots in Fig. 4 that are spatially aligned with the axial location of the screw mixer and located directly underneath the position projections are the tracer particle's transverse and axial speed, respectively. This visualization method allows the relationship between the tracer particle's position and speed to be made at each point throughout the screw mixer. As previously mentioned, the LOESS algorithm was applied to the speed data to improve its visualization [19].

To determine if the granular flow structures are repeatable, three independent trials were conducted with a single tracer particle and the resulting position and speed profiles for the three trails were compared via qualitative visualization in addition to a quantitative evaluation of the variation in the dimensionless pathlength and dimensionless residence time. The position and speed profiles for three independent trials conducted at the reference condition are shown in Fig. 4. The standard deviation of the dimensionless pathlengths and dimensionless residence times were determined to be 4.4% and 5.8% of the average dimensionless pathlength and average dimensionless residence, thus quantitatively indicating a high degree of repeatability. These quantitative results will be shown in the following sections when comparing them to other operating conditions.

Fig. 4 indicates that the initial starting positions of the three tracer particles were slightly different between trials, depending on how the tracer particles were injected into the screw mixer and also how they encountered the screw mixer's geometrical features (e.g., screws) and the other granular materials. These differences in initial starting position result in the pathlines for the three different tracer particles to show some variation from trial to trial; however, despite these differences in position, several important characteristics of the tracer particle's position and speed profiles are very repeatable.

First, the tracer particles translate between screw one and screw two several times before finally leaving the screw mixer. This

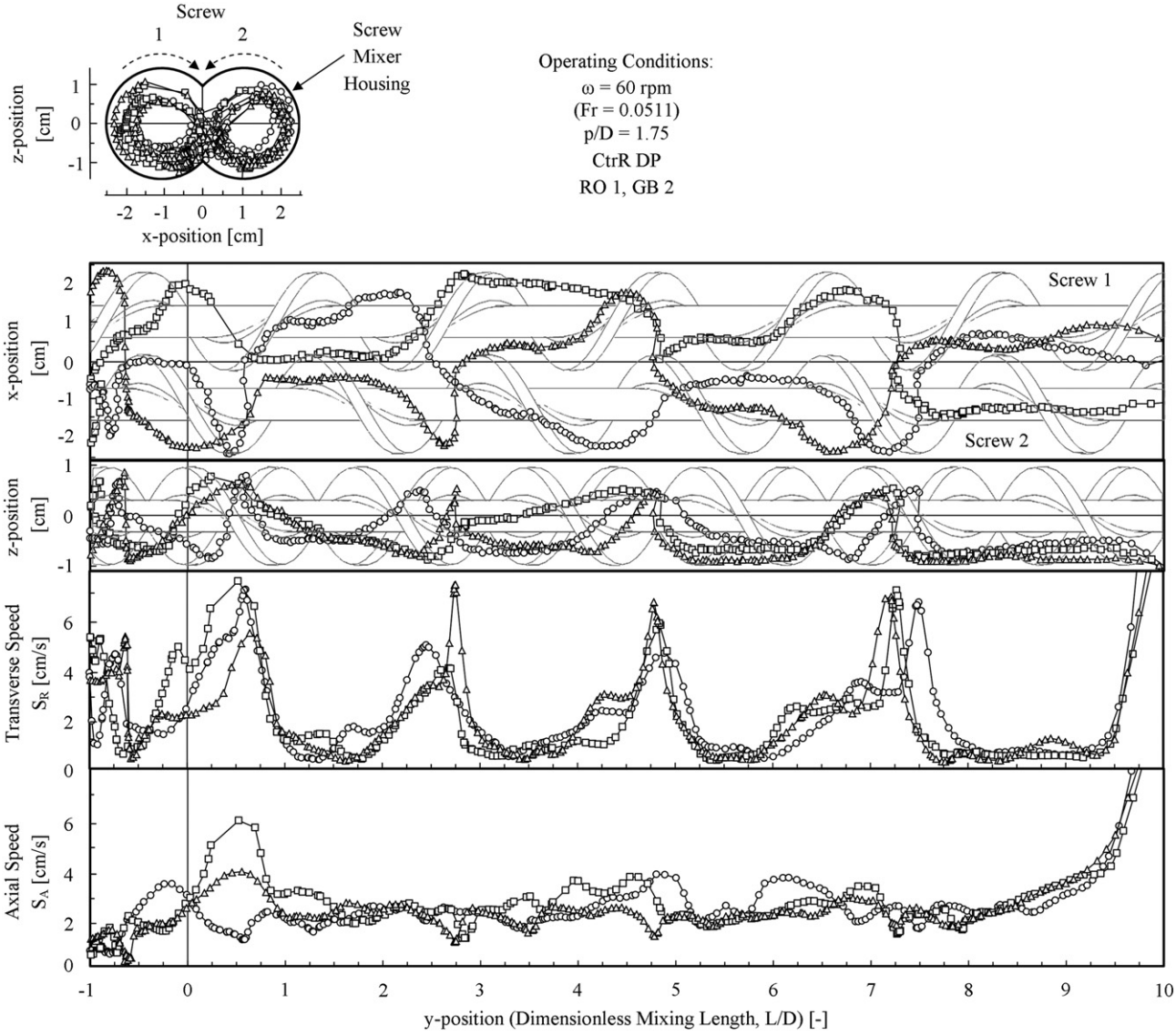

Fig. 4. Position and speed profile for three different tracer particles each from an independent trial for the reference condition (operating condition 7). Each symbol represents a different tracer particle.

behavior is easily visualized in the x–y projection, but can also be seen in the x–z projection. This behavior is beneficial in terms of the mixing effectiveness of the screw mixer because it illustrates a large amount of convective mixing by utilizing the entire mixing region of the screw mixer and inducing bulk granular flow throughout the screw mixer.

Second, the tracer particles undergo periodic fluctuations in the z-direction as they move through the screw mixer, as shown in the y–z projection. The peaks in the z-direction represent locations where the tracer particles are being lifted up toward the top surface of the granular mixture. These locations are also aligned with instances when the tracer particles are experiencing a large shift in the x-position, as shown in the x–y projection, either in the positive direction when near screw one, or in the negative direction when near screw two. In both cases, the tracer particle is being translated in the horizontal direction toward the middle of the screw mixer (i.e., the region between the two screws), which is a result of the counter-rotating down-pumping screw rotation orientation. This large translation in the x-direction occurs when the tracer particle reaches the top surface of the granular materials because there are fewer particle-particle contacts. The tracer particle translation results in a significant increase in the transverse speed of the tracer particle at locations of L/D ≈ 0.5, 2.7, 5.0, and 7.4. Thus, for this operating condition, the tracer particles behave in a somewhat periodic manner with an average period equivalent to L/D ≈ 2.3. In contrast, when the tracer particle is located in the bottom half of the screw mixer (i.e. below the mid-plane of the screw shafts), the transverse speed is extremely small as a result of the increased particle concentration and particle–particle contacts.

Third, the axial speed of the tracer particles remains fairly constant, at least in the range from L/D = 1 to L/D = 9. Prior to L/D = 1, the tracer particles undergo a very chaotic process because of the entrance effects associated with the absence and injection of the glass beads prior to and at L/D = 0, respectively. This behavior is observed in the tracer particle's x–y and y–z position projections and both of the speed graphs by its large fluctuations.

Finally, as the tracer particle reaches the end of the screw mixer, its axial and transverse speed dramatically increases. This behavior is a result of the discharge of the granular material to the outlet ports which causes a more free-flowing mixture. The different behavior of the tracer particle near the beginning and end of the mixing region essentially causes “entrance” and “exit” effects to be introduced. Overall, the three independent trials that were conducted feature very similar granular flow structures indicating a high degree of repeatability.

In addition to the three independent trials conducted for the reference conditions, three independent trials were also conducted for the remaining seven operating conditions used in this study. The average dimensionless pathlength and dimensionless residence time of the three trials will be presented in the following sections and the standard deviation of the three trials will be shown to provide a quantitative depiction of the repeatability of the results. However, due to the complexity of simultaneously visualizing and describing multiple tracer particle pathlines and the repeatable characteristics between different trials, only one of the three trials' position and speed profiles are shown in the following sections.

3.2. Screw rotation speed

The dimensionless pathlength and dimensionless residence time of the tracer particle in the effective mixing region (0 < L/D < 10) was measured for each of the trials that were performed for each operating condition. The average dimensionless pathlength and average dimensionless residence time as a function of screw rotation speed through the use of the Froude number, holding all other parameters constant, is shown in Fig. 5. The left and right y-axes represent the dimensionless pathlength and dimensionless residence time,

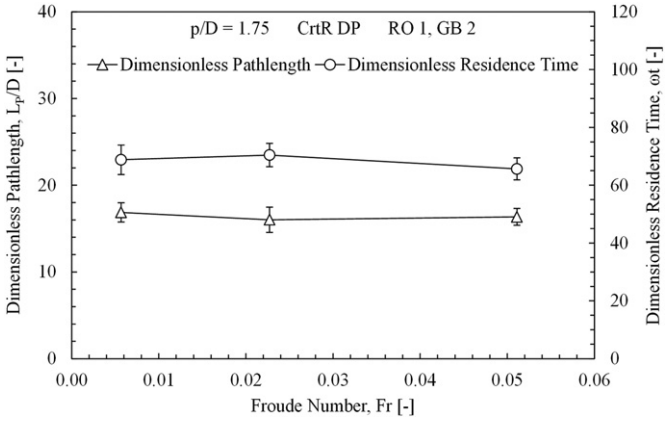

Fig. 5. Dimensionless pathlength and dimensionless residence time as a function of Froude number.

respectively. The vertical error bars represent plus and minus one standard deviation that was computed from the three separate trials. Note that the error bars are fairly small, emphasizing the minimal variations from trial to trial. As shown, the dimensionless pathlength and dimensionless residence time of the tracer particle was independent of the Froude number, suggesting that the granular flow structures are similar. To visually demonstrate these similarities, the resulting tracer particle position and speed profiles that were obtained by maintaining all the same operating conditions as the reference condition, except the screw rotation speed which was changed to ω = 20 rpm (operating condition 1), resulting in a Froude number of Fr = 0.0057, are shown in Fig. 6.

Relative to the reference condition, the pathline of the tracer particle looks quite similar. The tracer particle makes frequent changes between the two screw regions, before leaving the screw mixer. Moreover, the tracer particle undergoes similar periodic fluctuations in the z-direction. In contrast to the similar pathline of the tracer particle, the speed profile for a screw rotation speed of ω = 20 is slightly different than for the ω = 60 case, as expected. In particular, the peaks in the transverse speed appear to be lower in magnitude. The axial speed remains fairly constant, as was the case for the reference condition; however, the overall magnitude is lower due to the slower screw rotation speed.

This similar behavior in the 3D granular flow structures between screw rotation speeds of ω = 20 and ω = 60 confirms previous qualitative observations reported by Kingston and Heindel [2] who noted that the granular mixing dynamics appeared to be fairly independent of the screw rotation speed when observing the mixing behavior using optical visualization.

3.3. Dimensionless screw pitch

Unlike the screw rotation speed, the dimensionless pathlength and dimensionless residence time are dependent on the dimensionless screw pitch, as shown in Fig. 7. The dimensionless pathlength is the largest for the dimensionless screw pitch of p/D = 1.75 and is significantly reduced for both p/D = 0.75 and 1.25. This indicates that for p/D = 1.75, the tracer particle is traveling further in the transverse plane. Despite the tracer particle traveling a longer distance for p/D = 1.75, the dimensionless residence time of the tracer particle is significantly higher for p/D = 0.75 than it is for p/D = 1.25 and 1.75. This behavior arises because the axial distance traveled by the tracer particle during a single rotation of the screws for p/D = 0.75 is shorter than for p/D = 1.25 and 1.75, resulting in a higher dimensionless residence time. However, as dimensionless screw pitch increases from p/D = 1.25 to 1.75, the dimensionless residence time remains relatively constant because the pathlength of the tracer particle in the screw mixer for p/D = 1.75 is also increasing. The influence of dimensionless screw

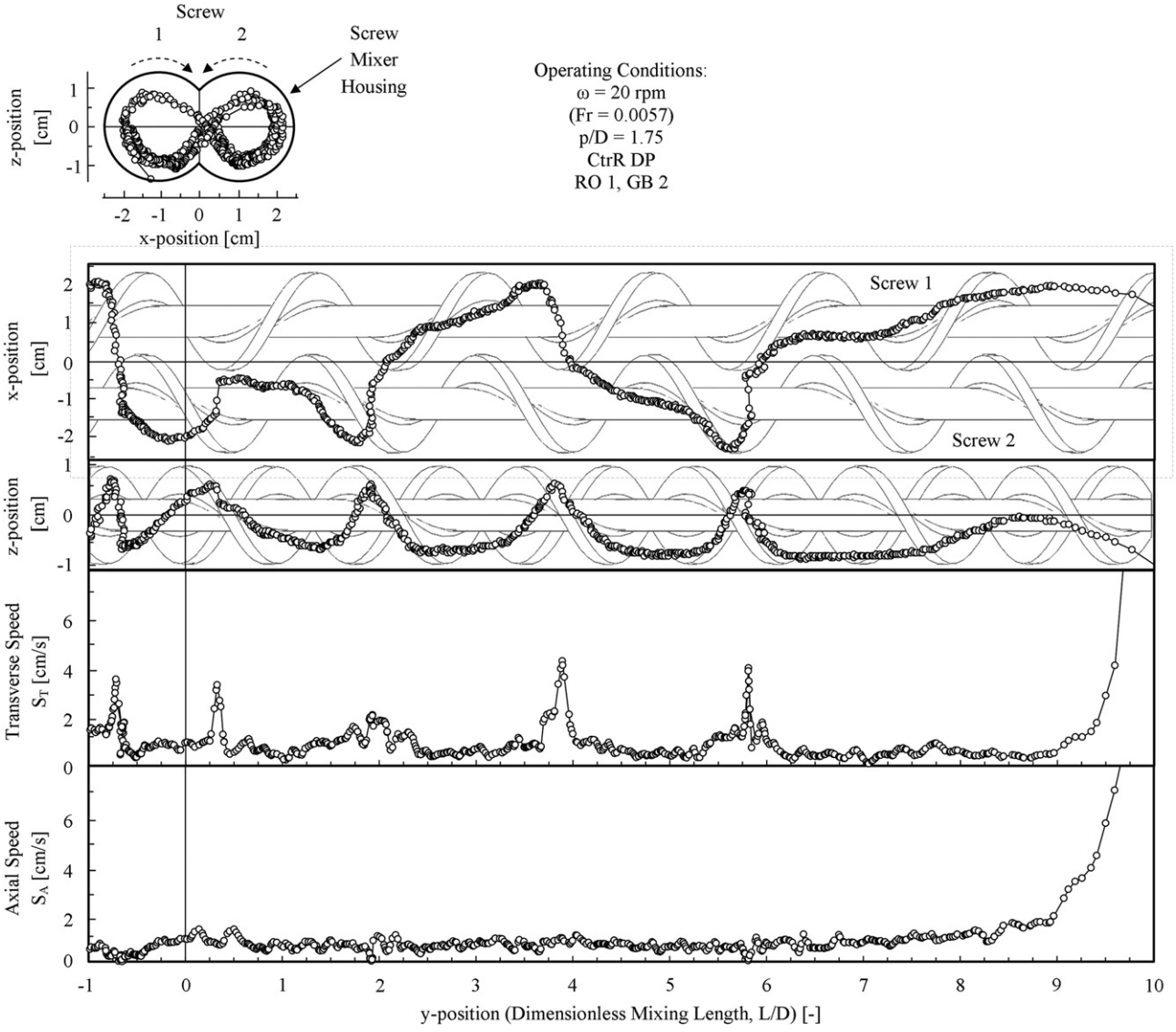

Fig. 6. The tracer particle's position and speed profile for a screw rotation speed of ω = 20 rpm (Fr = 0.0057).

pitch has also been shown to have significant implications in the diffusion coefficient of powder mixing, as report by Uchida and Okamoto [30].

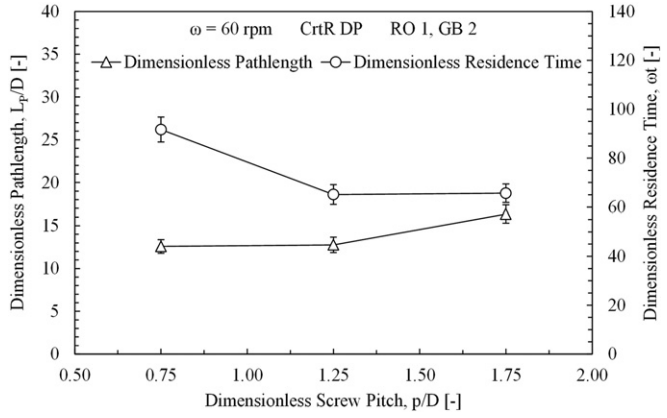

Fig. 7. Dimensionless pathlength and dimensionless residence time as a function of the dimensionless screw pitch.

Investigation into the tracer particle position and speed profiles provides critical insight into the changes in the granular flow structures for different levels of the dimensionless screw pitch. As shown in Fig. 8, when the screw mixer was operated with a dimensionless screw pitch of p/D = 0.75, the tracer particle did not translate back and forth between the two different screw regions. Instead, it circulated around screw one for the duration of the test. This behavior is most easily visualized in the x–z and x–y projections. Each of the three trials that were performed for this operating condition featured the same behavior. This behavior leads to the conclusion that a double screw mixer with a dimensionless screw pitch of p/D = 0.75 actually behaves as two single screw conveyors and the lack of transverse motion around both of the screws is believed to result in a less effective mixing process, as was noted by Kingston and Heindel [2]. Furthermore, the periodic movement of the tracer particle around the screw occurred at approximately half the frequency as the reference condition, which is analogous to the reduced frequency in the sine-like pathline noted by Uchida and Okamoto [30] for small dimensionless screw pitches in single screw mixer applications.

Similar to the reference condition, the axial speed of the tracer particle remained fairly constant throughout the screw mixer. However, the exit effects did not become apparent until closer to the end of the screw mixer, which occurred at approximately L/D = 9.5. This is a

characteristic of the changing screw flighting angle and increasing number of screw flights that results from shortening the dimensionless screw pitch, relative to the reference condition. These results confirm the findings that longer dimensionless screw pitches cause the entrance and exit effects to propagate further into the screw mixer, which was proposed by Kingston and Heindel [31] in their investigation of the mixing effectiveness as a function of the dimensionless mixing length of the screw mixer.

3.4. Screw rotation orientation

The dimensionless pathlength and dimensionless residence time were significantly influenced by the screw rotation orientation, as shown in Fig. 9. Additionally, a proportional relationship between the dimensionless pathlength and the dimensionless residence time exits when changing the screw rotation orientation, in contrast to the behavior observed for the dimensionless screw pitch. Changing from a counter-rotating down-pumping (CtrR DP) screw rotation orientation to either a counter-rotating up-pumping (CtrR UP) or co-rotating (CoR) screw rotation orientations resulted in a significant reduction in the dimensionless pathlength and dimensionless residence time. The longer dimensionless residence time associated with the counter-rotating down-pumping screw rotation orientation was attributed to the increased dimensionless pathlength resulting from the tracer

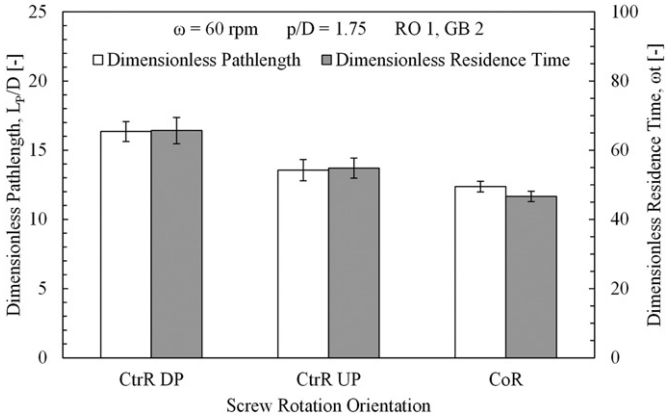

Fig. 9. Dimensionless pathlength and dimensionless residence time as a function of the screw rotation orientation.

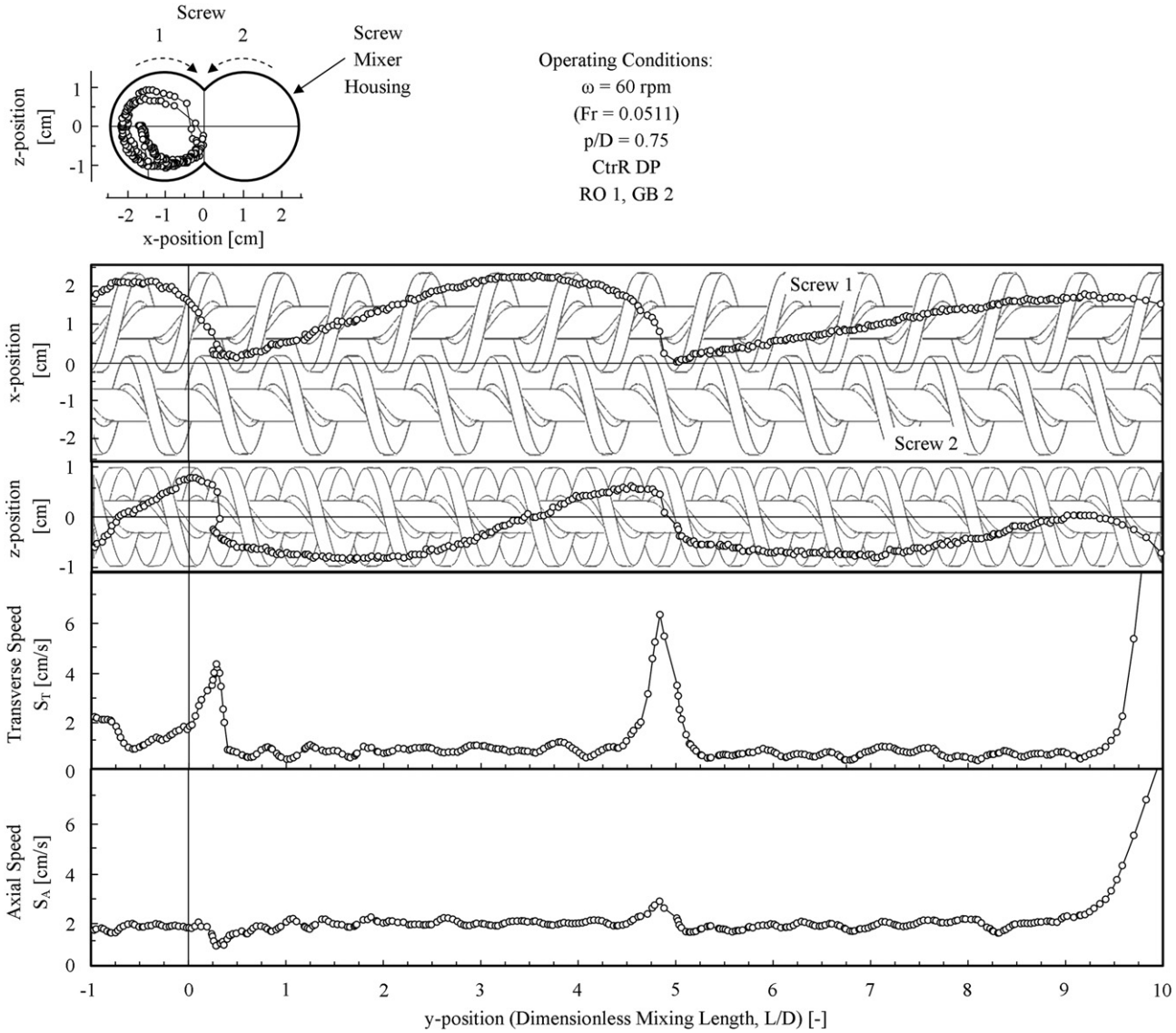

Fig. 8. The tracer particle's position and speed profile for a dimensionless screw pitch of p/D = 0.75.

particle to be transmitted back and forth between the two screws. This outcome provides significant insight into a critical phenomenon that was noted by Kingston and Heindel [2], who discovered that a counter-rotating down-pumping screw rotation orientation offered significant improvements in terms of the mixing effectiveness of the screw mixer.

A counter-rotating up-pumping (CtrR UP) screw rotation orientation resulted in similar behavior to that of, surprisingly, the dimensionless screw pitch of p/D = 0.75. More specifically, the tracer particle exhibited very little movement between the two screws, as shown in Fig. 10. In fact, the only time the tracer particle moved from the region near screw one to screw two was before it reached the effective mixing region, after which it stayed near screw two for the duration of the test. This lack of translational motion between the two screws explains why the dimensionless pathlength and dimensionless residence time was reduced for the counter-rotating up-pumping screw rotation orientation.

Previous studies by Kingston and Heindel [2] showed that a co-rotating double screw mixer does not provide advantageous mixing performance relative to a counter-rotating down-pumping screw rotation orientation. However, characterizing co-rotating configurations is still valuable because they are utilized in many industrial applications. Furthermore, characterization also provides insight into why the co-rotating screw rotation orientation resulted in shorter dimensionless pathlengths and a reduced dimensionless residence time. As shown in Fig. 11, changing the screw rotation orientation to a co-rotating (CoR) configuration resulted in significant changes in the granular flow structure of the tracer particle. First, it caused the tracer particle to reverse its trajectory multiple times instead of moving in a continuous pathline as it did in the reference condition. This effect is most easily visualized in the x–z projection shown in Fig. 11. The tracer particle first begins near screw one, and is then transmitted toward the right and down between the screws. As the tracer particle moves to the right and below screw two, the tracer particle reverses its trajectory and begins to move back toward the middle of the screw mixer before it is brought up to the top surface of the granular bed and rotated around screw two. It is proposed that this behavior would have a negative impact on the granular mixing process because it causes the granules to become temporarily stagnant and exhibit minimal mixing. Second, the tracer particle floats on top of the granular bed in between screw two and the screw mixer housing, from approximately L/D = 5 to L/D = 7, as shown in the x–y and x–z projections. Large red oak chip agglomerations were noted to frequently occur in this region of the screw

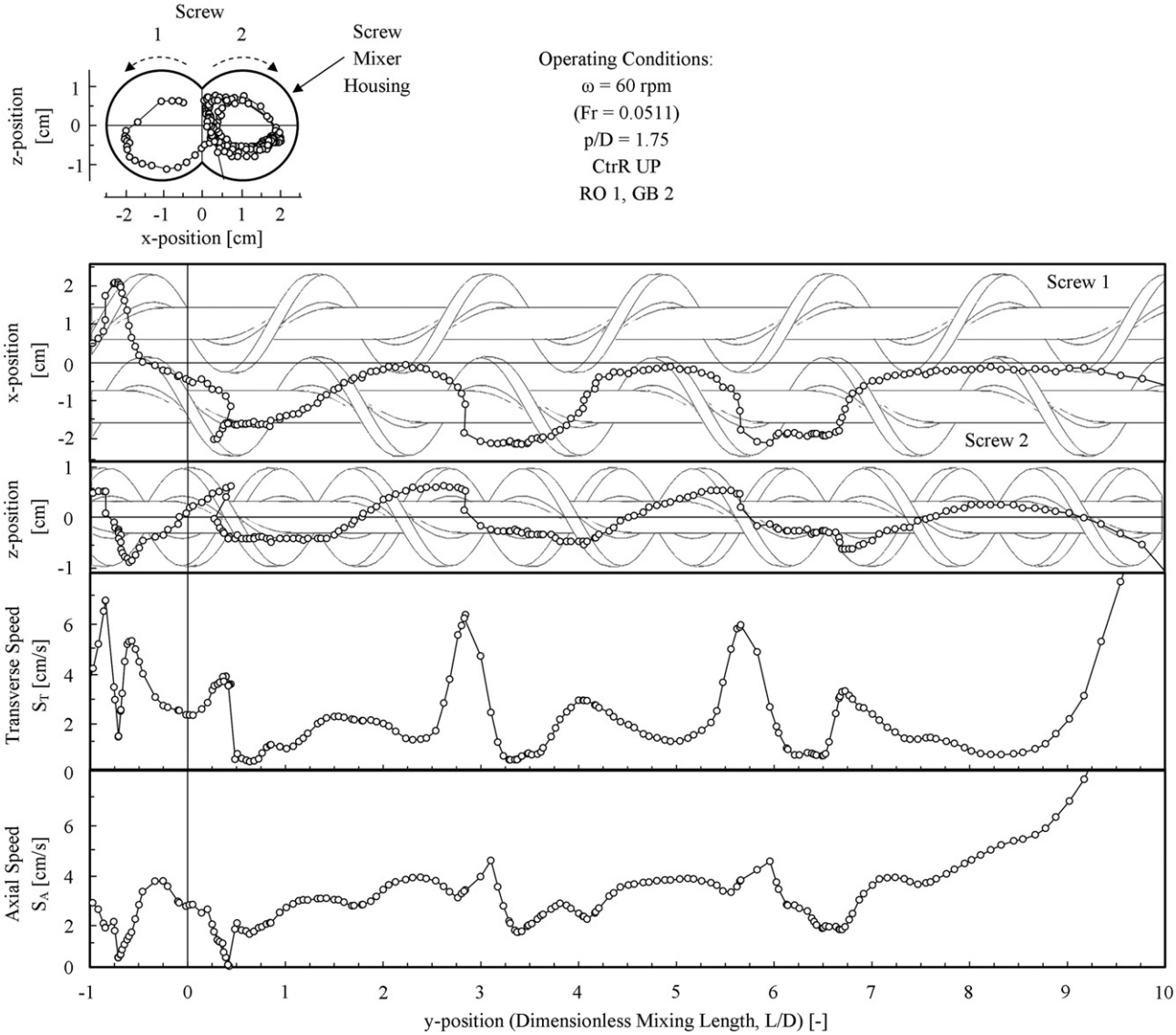

Fig. 10. The tracer particle's position and speed profile for a counter-rotating up-pumping (CtrR UP) screw rotation orientation.

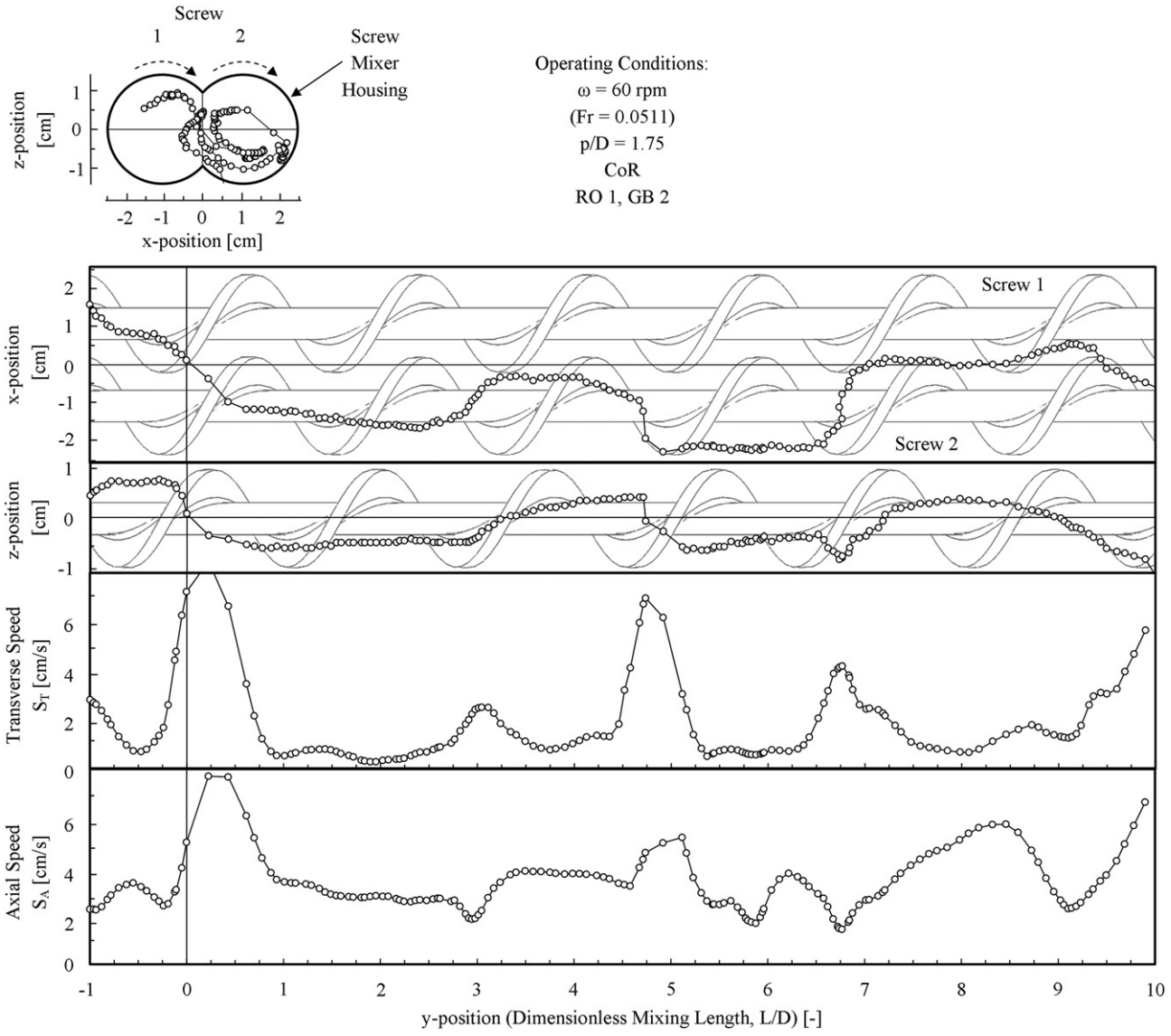

Fig. 11. The tracer particle's position and speed profile for a co-rotating (CoR) screw rotation orientation.

mixer in Kingston and Heindel's [2] previous studies, and ultimately resulted in decreased mixing performance.

In terms of the transverse speed of the tracer particle, a co-rotating screw rotation orientation displays few changes relative to the reference condition. However, the axial speed of the tracer particle showed signs of periodic fluctuations, which were not found in the reference case. Moreover, there is a considerable increase in the magnitude of the axial speed, on average, throughout the screw mixer, which partly attributes to the reduced dimensionless residence time.

3.5. Material injection configuration

Changing the material injection configuration had a relatively small influence on the dimensionless pathlength and dimensionless residence time, as shown in Fig. 12. When the material injection configuration was changed from the red oak chips and glass beads being injected in port one and two (RO 1, GB 2), respectively, to the red oak chips and glass beads being injected into port two and one (RO 2, GB 1), respectively, only a slight reduction in the dimensionless pathlength and dimensionless residence time was observed. However, these differences are comparable to the variation between the different trials; thus, these two conditions cannot be distinguished. However, to provide some insight into why a small

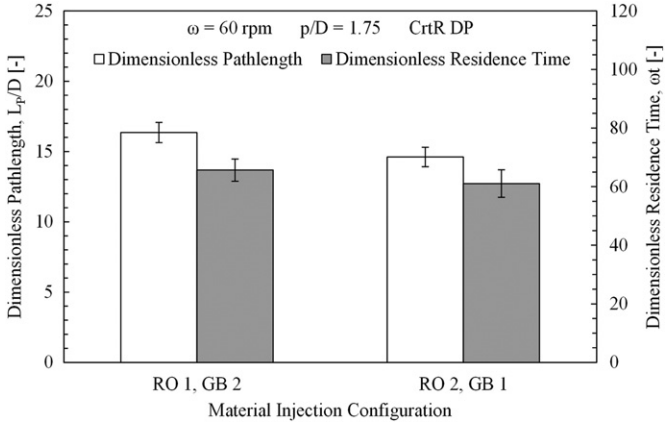

Fig. 12. Dimensionless pathlength and dimensionless residence time as a function of the material injection configuration.

difference may be present, the tracer particle position and speed profile is shown in Fig. 13.

The most noticeable effect on the granular flow structures resulting from the change in the material injection configuration came in the form of increased entrance effects associated with the tracer particle's transverse and axial speed, as shown in Fig. 13. As the tracer particle was being injected into the screw mixer through injection port two for this condition, at approximately L/D = 0, it had a large speed as a result of the free-fall from the volumetric feeders, and propagated about one dimensionless mixing length into the screw mixer. A result of this high initial speed is a slightly reduced dimensionless pathlength and dimensionless residence time.

4. Conclusions

Previous studies in the literature have visualized the effect of operating conditions and mixer geometry on the resulting 2D flow structures in single and double screw mixers. In this study, the 3D granular flow structures inside a double screw mixer were characterized using XPTV and shown to be significantly influenced by the selected operating conditions. The dimensionless pathlength and dimensionless residence time was shown to be independent of Froude number and similar pathline characteristics were qualitatively observed. The counter-rotating down-pumping screw rotation orientation resulted in increased dimensionless pathlengths and dimensionless residence times relative to the other two screw rotation orientations. This behavior is projected to increase the mixing effectiveness of the screw mixer by providing a more convective mixing process, which is consistent with the findings of Kingston and Heindel [2]. Significant quantitative differences were not observed for the two different material injection configurations although qualitative observations indicated that injecting red oak chips and tracer particles into the downstream injection port slightly inflated the entrance effects.

Most commonly, an increase in the dimensionless pathlength resulted in an increase in the dimensionless residence time. However, tests performed at different dimensionless screw pitches indicated a tradeoff between the dimensionless pathlength and dimensionless residence time exists when changing this parameter. Since previous studies by Kingston and Heindel [2] demonstrated that a dimensionless screw pitch of p/D = 1.75 resulted in increased mixing performance and this study showed that this operating condition was accompanied with longer dimensionless pathlengths but shorter dimensionless residence times, it is proposed that the length of the dimensionless pathlength provides a better prediction of the mixing performance of the system because of its ability to characterize the degree of granular motion and convective mixing.

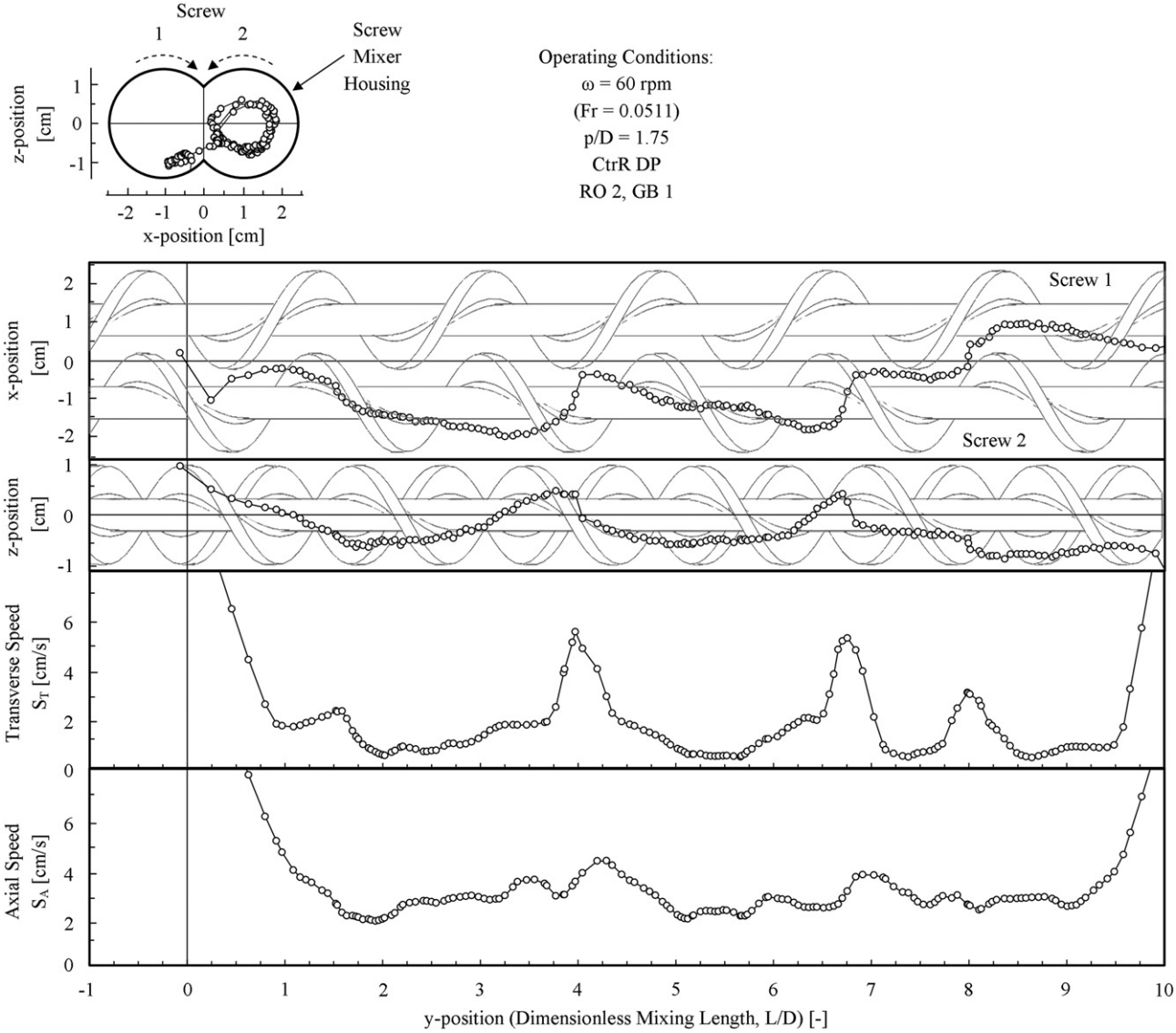

Fig. 13. The tracer particle's position and speed profile for a material injection configuration with the red oak chips and glass bead injected into port one and two, respectively.

Acknowledgments

Support for portions of this work by the Phillips 66 Company is gratefully acknowledged. The X-ray facility used in this research was funded by the National Science Foundation under award number CTS-0216367 and Iowa State University.

References

[1] T.A. Kingston, T.J. Heindel, Optical visualization and composition analysis to quantify continuous granular mixing processes, Powder Technol. 262 (2014) 257–264.
[2] T.A. Kingston, T.J. Heindel, Granular mixing optimization and the influence of operating conditions in a double screw mixer, Powder Technol. 266 (2014) 144–155.
[3] A.A. Aissa, C. Duchesne, D. Rodrigue, Polymer powders mixing part I: mixing characterization in rotating cylinders, Chem. Eng. Sci. 65 (2010) 786–795.
[4] A.A. Aissa, C. Duchesne, D. Rodrigue, Polymer powders mixing part II: multi-component mixing dynamics using RGB color analysis, Chem. Eng. Sci. 65 (2010) 3729–3738.
[5] B. Daumann, H. Nirschl, Assessment of the mixing efficiency of solid mixtures by means of image analysis, Powder Technol. 182 (2008) 415–423.
[6] B. Daumann, A. Fath, H. Anlauf, H. Nirschl, Determination of the mixing time in a discontinuous powder mixer by using image analysis, Chem. Eng. Sci. 64 (2009) 2320–2331.
[7] D.R. Van Puyvelde, B.R. Young, M.A. Wilson, S.J. Schmidt, Experimental determination of transverse mixing kinetics in a rolling drum by image analysis, Powder Technol. 106 (1999) 183–191.
[8] K. Uchida, K. Okamoto, Measurement of powder flow in a screw feeder by X-ray penetration image analysis, Meas. Sci. Technol. 17 (2006) 419–426.
[9] Y.J. Gao, A. Vanarase, F. Muzzio, M. Ierapetritou, Characterizing continuous powder mixing using residence time distribution, Chem. Eng. Sci. 66 (2011) 417–425.
[10] A.U. Vanarase, F.J. Muzzio, Effect of operating conditions and design parameters in a continuous powder mixer, Powder Technol. 208 (2011) 26–36.
[11] G.R. Ziegler, C.A. Aguilar, Residence time distribution in a co-rotating, twin-screw continuous mixer by the step change method, J. Food Eng. 59 (2003) 161–167.
[12] J. Chaouki, F. Larachi, M.P. Dudukovic, Noninvasive tomographic and velocimetric monitoring of multiphase flows, Ind. Eng. Chem. Res. 36 (1997) 4476–4503.
[13] T.J. Heindel, A review of X-ray flow visualization with applications to multiphase flows, J. Fluids Eng. Trans. ASME 133 (2011).
[14] J.B. Drake, N.P. Franka, T.J. Heindel, X-ray particle tracking velocimetry for applications in fluidized beds, ASME International Mechanical Engineering Congress and Exposition, Boston, Massachusetts, USA, 2008 (Paper No. IMECE2008-66224).
[15] S.J. Lee, G.B. Kim, X-ray particle image velocimetry for measuring quantitative flow information inside opaque objects, J. Appl. Phys. 94 (2003) 3620–3623.
[16] S.J. Lee, G.B. Kim, D.H. Yim, S.Y. Jung, Development of a compact X-ray particle image velocimetry for measuring opaque flows, Rev. Sci. Instrum. 80 (2009).
[17] A. Seeger, U. Kertzscher, K. Affeld, E. Wellnhofer, Measurement of the local velocity of the solid phase and the local solid hold-up in a three-phase flow by X-ray based particle tracking velocimetry (XPTV), Chem. Eng. Sci. 58 (2003) 1721–1729.
[18] T.B. Morgan, T.J. Heindel, X-ray particle tracking of dense particle motion in a vibration-excited granular bed, ASME International Mechanical Engineering Congress and Exposition — 2010, Vol 7, Pts A and B2010. 1709–1717.
[19] T.A. Kingston, T.B. Morgan, T.A. Geick, T.R. Robinson, T.J. Heindel, A cone-beam compensated back-projection algorithm for X-ray particle tracking velocimetry, Flow Meas. Instrum. 39 (2014) 64–75.
[20] J.N. Brown, R.C. Brown, Process optimization of an auger pyrolyzer with heat carrier using response surface methodology, Bioresour. Technol. 103 (2012) 405–414.
[21] L. Ingram, D. Mohan, M. Bricka, P. Steele, D. Strobel, D. Crocker, B. Mitchell, J. Mohammad, K. Cantrell, C.U. Pittman, Pyrolysis of wood and bark in an auger reactor: physical properties and chemical analysis of the produced bio-oils, Energy Fuel 22 (2008) 614–625.
[22] S. Thangalazhy-Gopakumar, S. Adhikari, H. Ravindran, R.B. Gupta, O. Fasina, M. Tu, S.D. Fernando, Physiochemical properties of bio-oil produced at various temperatures from pine wood using an auger reactor, Bioresour. Technol. 101 (2010) 8389–8395.
[23] H.J. Park, H.S. Heo, Y.K. Park, J.H. Yim, J.K. Jeon, J. Park, C. Ryu, S.S. Kim, Clean bio-oil production from fast pyrolysis of sewage sludge: effects of reaction conditions and metal oxide catalysts, Bioresour. Technol. 101 (2010) S83–S85.
[24] H. Colijn, Mechanical Conveyors for Bulk Solids, Elsevier Science Publishers B.V, Amsterdam, New York, 1985.
[25] T.J. Heindel, J.N. Gray, T.C. Jensen, An X-ray system for visualizing fluid flows, Flow Meas. Instrum. 19 (2008) 67–78.
[26] W. Dos Passos, Numerical Methods, Algorithms, and Tools in c#, Taylor & Francis, 2011.
[27] W.S. Cleveland, Robust locally weighted regression and smoothing scatterplots, J. Am. Stat. Assoc. 74 (1979) 829–836.
[28] W.S. Cleveland, S.J. Devlin, Locally weighted regression — an approach to regression analysis by local fitting, J. Am. Stat. Assoc. 83 (1988) 596–610.
[29] D. Mohan, C.U. Pittman, P.H. Steele, Pyrolysis of wood/biomass for bio-oil: a critical review, Energy Fuel 20 (2006) 848–889.
[30] K. Uchida, K. Okamoto, Measurement technique on the diffusion coefficient of powder flow in a screw feeder by X-ray visualization, Powder Technol. 187 (2008) 138–145.
[31] T.A. Kingston, T.J. Heindel, Characterizing granular mixing homogeneity at various dimensionless mixing lengths in a double screw mixer, ASME Fluids Engineering Division Summer Meeting, Chicago, Illinois, 2014 (Paper No. FEDSM2014-21048).